and consequently indistinguishable from a small decrease in the planet's radius. Any lack of precision in the determination of c in terms of terrestrial units (such as km/sec) is clearly irrelevant to our experiment since time delays only are of concern.

In making the time-delay measurements, a radar cannot be directed towards the solar limb because of the radio interference that would result. For the Haystack facility, however, the antenna beam width is sufficiently narrow and the near side lobes of sufficiently low gain that the beam can be directed well within a degree of the limb without the solar radio emanations introducing a significant increase in the overall system noise temperature. For Arecibo the closest possible approach is about 1°. Were both inner planets to have the same ratio of radar to geometric cross section, then at superior conjunction Venus would always be more easily detected, the received power being about a factor of two greater. However, at the X-band frequency of Haystack, Venus may very well have a relatively low radar cross section[10] because of absorption in its atmosphere.

Although Mercury passes through superior conjunction about once in four months, some passages are considerably more useful than others from the points of view of ease of detectability and of close angular approach to the sun. The most favorable in the next two years occur on 11 June 1965 and 27 May 1966; in the former the minimum angular distance is about 1° and in the latter about 0.5°. The superior conjunctions of Venus are less variable and usually lead to an angular distance of closest approach of about 1°, as in the next two which will be on 12 April 1965 and 9 November 1966. The second occurs in southern declinations and so will be invisible to the Arecibo radar whose antenna is not steerable.

*Operated with support from the U. S. Air Force.

[1]In an interplanetary radar experiment, the Doppler shift of the radar wave is also measured; but although the effect on time delay of the change in c is cumulative, the corresponding general relativistic effect on Doppler cancels out over the round trip.

[2]J. V. Evans and G. H. Pettengill, private communication.

[3]See, for example, P. G. Bergmann, Introduction to the Theory of Relativity (Prentice-Hall, Inc., Englewood Cliffs, New Jersey, 1942), p. 203.

[4]In an earth-moon experiment, however, the relativistic contribution to the difference in measured time delay between new and full moon is quite undetectable, being only about 5×10^{-11} sec.

[5]With measurements extended over a several-year period the precession of Mercury's perihelion could also be estimated accurately and independently of the optical data; in addition, reasonably strict limits could be placed on the possible time dependence of G.

[6]W. C. Erickson, Astrophys. J. 139, 1290 (1964).

[7]The only other facility that could now participate significantly in this measurements program is Jet Propulsion Laboratory's Goldstone radar, operated at a frequency of 2388 Mc/sec.

[8]With one of these frequencies at about 400 Mc/sec or lower, the integrated electron density along the path of the radar wave could be determined accurately, thus providing useful information on the solar corona. Faraday rotation effects may also shed light on certain characteristics of the solar magnetic field.

[9]I. I. Shapiro, to be published.

[10]D. Karp, W. E. Morrow, Jr., and W. B. Smith, to be published.

ION TRAPPING IN ROTATING HELIUM II

R. L. Douglass
Physics Department, American University of Beirut, Beirut, Lebanon
(Received 5 November 1964)

Trapping of negative ions in the cores of quantized vortex lines has been suggested by Careri, McCormick, and Scaramuzzi[1] as an explanation for their discovery of rotation-induced attenuation of space-charge limited ion currents in He II. This Letter reports the direct detection of trapped negative ions in rotating He II, and some measurements of their mean trapped time and of their mobility parallel to the rotation axis at temperatures between 1.20 and 1.72°K. No evidence of positive-ion trapping has been found, in agreement with the ion-current measurements,[1,2] and in contrast to the experiment of Rayfield and Reif[3] at much lower temperatures.

The He II is contained in an electrode assem-

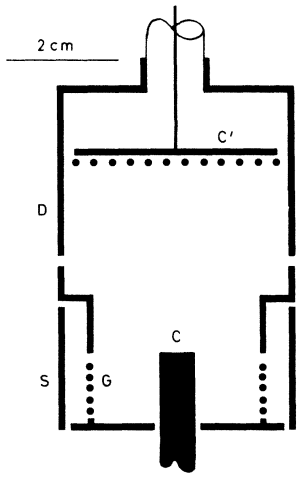

FIG. 1. Vertical cross section of the rotating electrode assembly. The Teflon insulators between electrodes have not been shown.

bly whose cross section is shown in Fig. 1. Alpha particles from Po^{210} deposited on the source electrode S produce a thin layer of ionization near S. Helium ions of either sign can be drawn through the control grid G to the collector C, or the ion current to C can be completely cut off. Current collected at C can be measured with a vibrating-capacitor electrometer. Above this triode section is a grounded drift chamber D and, above a grounded "Frisch grid," another collector C'. All electrodes have rough silver-plated surfaces. The Teflon separating the electrodes has been kept to a minimum to reduce any possibility of electrostatic charge accumulation on insulators. The potentials of S, G, C, and C' can be independently controlled while the assembly rotates.

In operation, an ion current is established through G to collector C and then, by appropriately changing potentials, the current from S is cut off and the space charge between G and C is flushed upward, some of it arriving on C'. The collector C' is rigidly connected to the floating grid of an electrometer-tube cathode follower whose output voltage is proportional to the charge collected. This voltage, after dc amplification, is displayed on an oscilloscope and photographed. Figure 2 shows sample traces. The switching of potentials which starts the flush of ions to C' is coupled by interelectrode capacity to C', producing the initial step seen on all traces.

In nonrotating He II, the vertical transit times,

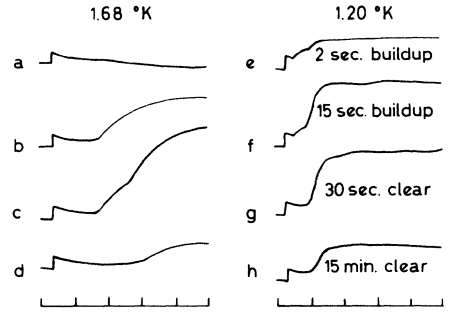

FIG. 2. Ion pulses at collector C'. Trace b was obtained in nonrotating helium; all others at 10 rpm. Horizontal units are seconds. Further explanations are given in the text.

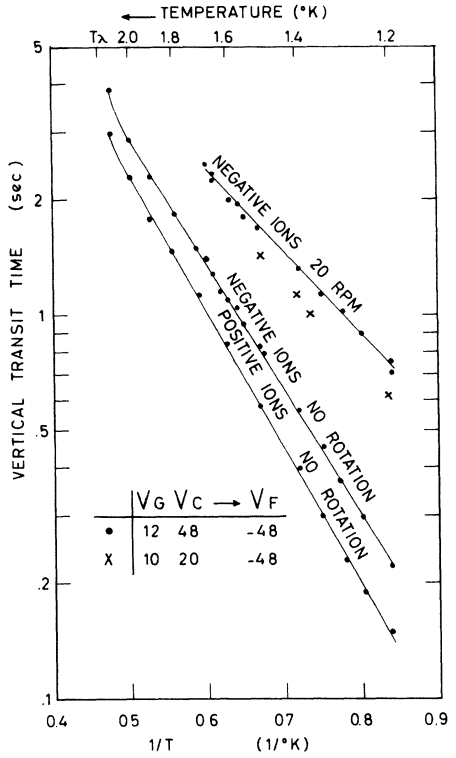

FIG. 3. Temperature dependence of ionic transit times from the region between electrodes G and C to the collector C'. In the nonrotating state the transit times are proportional to $\exp(-\Delta/T)$ with $\Delta = 8.4$ and 7.7°K for positive and negative ions, respectively. The table shows the voltages of G and C before the flushup and the final potential of both during flushup for negative ions. For positive ions the signs are reversed.

measured from the step to the initial rise of the ion pulse [Fig. 2(b)], reflect the known exponential time dependences of the free-ion mobilities[4] (see lower curves of Fig. 3). At tem-

peratures below 1.72°K when the helium was rotating, the negative-ion pulses were changed by the appearance of a second pulse, superimposed on the first [Fig. 2(c)]. That this second pulse was due to trapped ions was demonstrated as follows: The ion current through G to C was cut off (by making S positive relative to G) for a period exceeding the G-to-C transit time (which is 1 sec or less). Then, when the ions remaining between G and C were flushed up to C', only the second pulse was observed [Fig. 2(d)]. No ion pulse was observed at C' unless the clearing period was preceeded by a negative-ion current flow through G to C [Fig. 2(a)]. The trapped-ion component of the pulse varies with the duration of the ion current. Figures 2(e) and 2(f) show pulses observed after 2 and 15 sec of ion current, respectively.

The well-defined difference in transit times of free and trapped ions shows that few of the trapped ions become free en route to C'. Thus the trapping structures must be continuous from top to bottom of the chamber, as is expected for vortex lines.

Figures 2(g) and 2(h) show trapped-ion pulses obtained after 30 sec of ion current followed, respectively, by 30-sec and 15-min clearing periods. During the entire clearing period the ions remain between G and C in the presence of horizontal fields exceeding 20 V/cm. By measuring trapped-ion pulse heights as a function of clearing time, the mean trapped time τ could be determined. At temperatures below 1.6°K, τ exceeds 10 min, but above 1.6°K it drops sharply to less than a second. In the region between 1.60 and 1.72°K our measurements (Fig. 4) are well represented by the relation

$$\tau \propto \exp(E_0/k_B T),$$

where k_B is Boltzman's constant and $E_0 = 0.012$ eV. We suggest that E_0 is associated with the depth of the potential well in which negative ions are trapped. We were unable to measure the mean trapped time at temperatures above 1.72°K, because it becomes shorter than the horizontal and vertical transit times.

On the vortex-line model one expects charge trapping to be proportional to angular velocity, i.e., to the predicted line density. At temperatures where the mean trapped time is short, the trapped-ion density quickly reaches an equilibrium with the free-ion density. At 1.68°K the equilibrium trapped-ion pulse height was, indeed, proportional to angular velocity up to

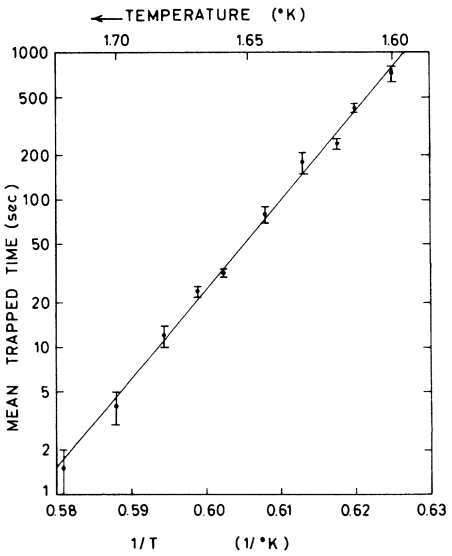

FIG. 4. The mean trapped times of negative ions in vortex lines. Each point is derived from a plot of the exponential decrease of trapped charge with clearing time.

45 rpm, the highest value tested.

At the lower temperatures, several minutes are required to reach equilibrium, and the trapped charge then becomes large enough to make a significant change in the field distribution between G and C. This is shown by a reduction in the ion current reaching C (due to space-charge limiting between G and C) and by a shortened trapped-ion transit time to C'. The latter effect is expected as a result of vertical spreading of the trapped charge cloud prior to flushup. Preliminary measurements indicate that, if the trapped-charge buildup is kept small, the trapped-ion pulse heights at 1.2°K are also proportional to angular velocity. Further study of ion trapping rates and possible saturation effects is underway and will be reported upon at a later date.

In order to keep the trapped negative ions vertically confined prior to flushing them upward, it was found necessary to keep grid G, as well as C, at a positive potential and to keep the trapped-ion density small. Under these conditions the vertical trapped-ion transit times were reproducible and independent of pulse height, and the leading edge of the trapped-ion pulse at C' was nearly as sharp as that of the free-ion pulse. The upper curve of Fig. 3 shows vertical transit times for the trapped-ion pulse. The trapped-ion transit times were independent of angular velocity (between 5 and 80 rpm) and

inversely proportional to the potential of G and C during flushout (between −20 and −100 V). The corresponding axial mobility of negative ions trapped in vortex lines is proportional to $\exp(\Delta/T)$ with $\Delta = 5.3 \pm 0.4$°K, and is perhaps one third of the free-negative-ion mobility at 1.2°K.

The absolute value of trapped-ion mobility cannot be accurately deduced by comparing free- and trapped-ion transit times to C' because free ions follow lines of force whereas trapped ions move only along vortex lines. Moreover, free and trapped ions may start upward from somewhat different heights between G and C. In equilibrium, the trapped ions will distribute themselves so that they are not subject to vertical fields. The location of the region of vanishing vertical field depends upon electrode potentials. The data points marked X, below the upper curve of Fig. 3, show the observed effect of a reduction in the potential V_C of collector C prior to flushup: The trapped ions float higher and their subsequent transit time to C' is reduced. For given electrode potentials, the transit times to C' are inversely proportional to mobilities, but the constants of proportionality are unknown and differ for free and trapped ions.

This work was supported in part by an institutional grant from the Rockefeller Foundation and a departmental grant from the Research Corporation.

[1]G. Careri, W. D. McCormick, and F. Scaramuzzi, Phys. Letters 1, 61 (1962).

[2]D. J. Tanner and R. J. Donnelly, Proceedings of the Ninth International Conference on Low Temperature Physics, Columbus, Ohio, 1964 (to be published).

[3]G. W. Rayfield and F. Reif, Phys. Rev. Letters 11, 303 (1963).

[4]F. Reif and Lothar Meyer, Phys. Rev. 119, 1164 (1960).

DISSIPATIVE MECHANISM IN TYPE-II SUPERCONDUCTORS

A. R. Strnad, C. F. Hempstead, and Y. B. Kim
Bell Telephone Laboratories, Murray Hill, New Jersey
(Received 2 November 1964)

Basic to the theory of type-II superconductors is Abrikosov's notion of the quantized flux lines, or vortices of superelectrons.[1] Such concepts as flux pinning, flux creep, and flux flow, that have been very useful in the understanding of hard superconductivity,[2] all envision the motion of Abrikosov flux lines. However, no satisfactory theoretical explanation has yet been advanced to account for the dissipative mechanism associated with the motion of flux lines. In this report we wish to direct theoretical interest to the simple, universal facts that have emerged from a large body of experimental data on the flux-flow state of type-II superconducting alloys.

Resistance in the mixed state has been measured with specimen geometry shown in Fig. 1. The upper critical field H_{c2} is determined resistively by orienting the externally applied magnetic field H parallel to the broad surfaces of the sample.[3] The resistance data reported here are, however, taken with H perpendicular to the sample surface. At a fixed field H, the voltage appearing in the direction of the current (longitudinal voltage) is measured as a function of current I. A detectable voltage appears when I exceeds the critical current; V then increases rapidly and becomes nearly linear in I. Although the critical currents vary considerably depending on the defect structure of the specimen, the slope $\Delta V/\Delta I$ in the linear region is found to be structure insensitive. In the upper figure are shown $V(I)$'s for two $Nb_{0.5}Ta_{0.5}$ samples containing different amounts of defects. From this observation, one would infer the $V(I)$ of a defect-free specimen to be the straight line passing through the origin. It is difficult in practice to prepare a sample in this ideal state, but its resistance can readily be determined from $\Delta V/\Delta I$ even in the presence of defects. We call the resistivity determined in this way the flow resistivity ρ_f. The structure-insensitive nature of ρ_f is further emphasized in the lower figure for two $Pb_{0.83}In_{0.17}$ samples. In one sample the copper plating has altered flux-pinning conditions (presumably on the surfaces) so as to increase the critical current at low fields but to decrease it at high fields. Note, however, that the flow resistivity at given field strength is practically